Understanding the infrared and Raman spectra of ganoderic acid A: An experimental and DFT study

Guohua Yao, Yuhan Ma, Muhammad Muhammad, Qing Huang

PII: S1386-1425(18)31016-3
DOI: https://doi.org/10.1016/j.saa.2018.11.019
Reference: SAA 16583
To appear in: *Spectrochimica Acta Part A: Molecular and Biomolecular Spectroscopy*
Received date: 11 August 2018
Revised date: 18 October 2018
Accepted date: 12 November 2018

Please cite this article as: Guohua Yao, Yuhan Ma, Muhammad Muhammad, Qing Huang , Understanding the infrared and Raman spectra of ganoderic acid A: An experimental and DFT study. Saa (2018), https://doi.org/10.1016/j.saa.2018.11.019

Understanding the infrared and Raman spectra of ganoderic acid A: An experimental and DFT study

Guohua Yao[a], Yuhan Ma[a,b,c], Muhammad Muhammad[a,c], Qing Huang[a,b,c,*]

[a] Key Laboratory of High Magnetic Field and Ion Beam Physical Biology, Institute of Technical Biology and Agriculture Engineering, Hefei Institutes of Physical Science, Chinese Academy of Sciences, Hefei 230031, China

[b] University of Science & Technology of China, Hefei, 230026, China

[c] College of Life Science, Anhui Science and Technology University, Fengyang 233100, China

*Corresponding author: Qing Huang

Email: huangq@ipp.ac.cn

Abstract

Ganoderic Acids (GAs) are the major medicinal compounds in *Ganoderma lucidum* used as traditional Chinese medicine since ancient times. Ganoderic acid A (GAA) is the first discovered ganoderic acids (GAs) reported in the literature, which is also one of most abundant triterpenoids of *Ganoderma lucidum*. Especially, GAA has been extensively investigated in recent decades for its positive medicinal activities. However, the vibrational properties of GAs have rarely been studied or reported. In this work, we focused on the typical GAA and studied the infrared (IR) and Raman spectra based on both experiments and DFT calculations. As such, we could not only achieve the assignments of the vibrational modes, but also from the IR and Raman spectra, we found that the spectral region from 1500 cm^{-1} to 1800 cm^{-1} is particularly useful for distinguishing different types of GAs. In addition, its dehydrogenated derivative ganoderenic acid A (GOA) was also studied, which could be identified due to its spectral feature of strong IR and Raman bands around 1620 cm^{-1}. This work therefore may facilitate the application of IR and Raman spectroscopy in the inspection and quality control of *Ganoderma lucidum*.

Keywords: Ganoderic Acids (GAs), Ganoderic Acid A (GAA), infrared spectroscopy, Raman spectroscopy, Ganoderenic acid A (GOA), DFT- M06-2X-D3

1. Introduction

Ganoderma lucidum (*G. lucidum*), namely, *Ling-Zhi* in Chinese and *Reishi* in Japanese, has been widely used as a well-known traditional medicinal mushroom for several thousand years in Asia due to its positive medicinal effects including improving immunity and promoting health [1, 2]. *G. lucidum* contains terpenoids, polysaccharides, proteins and small amounts of amino acids and vitamins as well. The pharmacological and clinical application of the aqueous/ethanol extracts of *G. lucidum* is prevention/treatment of various types of human diseases, such as allergy, bronchitis, hyperglycemia, inflammation, nephritis, hepatopathy, arthritis, hypertension, neurasthenia and chronic hepatitis [3].

Ganoderic acids (GAs), which are highly oxygenated C30 lanostane-type triterpenoids, are responsible for the pharmacological activities of *G. lingzhi* [4, 5]. Amongst terpenes and triterpenes, GAs are considered as one of major medicinal compounds in *G. lucidum*. Since 1982, a lot of studies found that GAs have antitumor activity, such as inhibiting proliferation of human cervical carcinoma, exhibiting cytotoxicity against hepatoma, suppressing growth and invasive behavior of breast cancer cells, inhibiting tumor growth and lung metastasis, inhibiting proliferation of prostate cancer and osteoclast differentiation [5-7]. Since the first isolation of GAA and GAB from *G. lucidum* by Kubota and Asaka [8], a series of GAs (like Ganoderma acid C, D, E, F… X, Y, Z, Df, DM, Me, Mk, et al.) have been isolated from the fruiting bodies, spores, and mycelia of *G. lucidum* and similar species, and there are more than one hundred isoforms of ganoderic acids which have been isolated and characterized [9-16]. While the basic lanosterol scaffold in the GAs remains the same, the side chains or functional units of different GAs vary and determine the function of particular ganoderic acid [17].

Ganoderic acid A (GAA) is the first discovered GA which is also one of the most abundant triterpenoids in *G. Lingzhi*, and it is generally concentrated in the Ganoderma genus. GAA exhibits hypolipidemic, antinociceptive, anti-inflammatory, antioxidative, hepatoprotective and anticancer activities [18-20]. Recently, GAA has gained special attention due to its apparent antitumour activities on human osteosarcoma, lymphoma, meningioma and breast cancer cells. It may become a promising candidate for new drug development [18].

Normally, GAs are separated through extraction and chromatography from *Ganoderma lucidum*, and then the molecular structures of the GA types can be determined by the techniques such as mass spectroscopy, NMR and X-ray diffraction [15, 18, 21]. The disadvantages of the methods of MS, NMR and X-ray diffraction are their instrumental expense and time-consuming operation. Nowadays, infrared (IR) spectroscopy and Raman spectroscopy gain more and more attention for their advantages in rapid, convenient measurements and fingerprint features. As far as we know, the analytical work of the IR and Raman spectra of GAs have not been reported. These vibrational spectra are very important in the structural analysis and spectral applications of biomolecules. For example, IR and Raman spectroscopy can be used as a marker for physiological process reactions in living organisms. In the different GAs (GAA, GAB, GAC, et al.), the great

extent of oxidative modification (with hydroxyl, oxo, acetoxyl group), especially at C3, C7, C12, C15, C22, C23 positions, are commonly observed in these skeletons [5, 16]. Since vibrational spectra can provide a lot of structural information and very sensitive to the chemical groups, vibrational spectra can thus be readily and effectively applied to identify the different types of GAs.

Therefore, in this work, we attempted to measure the IR and Raman spectra of GAs, and analyze the structures and types of GAs by combining vibrational spectroscopy experiments and DFT calculations. The vibration mode analysis of typical GAA can be used as a reference for analysis of other GAs. So in addition, based on the combined analysis of both the vibrational experimental spectra and the DFT theoretical calculations, other types of ganoderic acids would also be readily identified.

2. Materials and methods

2.1 Materials

Ganoderic acid A (Ganoderma acid A, GAA) and Ganoderenic acid A (noted as GOA, since its side chain is changed into the olefin chain relative to GAA) were purchased from Linyi Azeroth bioscience Co., Ltd. Ganoderic acid C (GAC) was purchased from Wuhan ChemFaces biochemical Co., Ltd. Potassium bromide (KBr) in spectral purity were purchased from Sinopharm Chemical Reagent Co., Ltd. Deionized water was prepared using a Millipore Milli Q-Plus system (Millipore, Bedford, MA, USA).

2.2 IR and Raman spectral measurements

For the IR measurements, the GAA or GOA powders were mixed with KBr and then pressed into pallets, respectively. The Fourier-Transform (FT)-IR spectra of the pallet samples were recorded in the range of 400 - 4000 cm^{-1} using the Alpha IR spectrometer (Bruker).

For the Raman spectral recording, the spectra with resolution ca. 3 cm^{-1} were taken in the 200-2000 cm^{-1} range using XploRA Raman spectrometer (HORIBA JOBIN YVON) excited with a 785 nm laser. The laser power was set at ca. 1.2 mW, and the acquisition time was 300 s.

3. Computational Details

DFT calculations were carried out using Gaussian 09 software [22]. The calculations in this work were performed by applying the functionals M06-2X-D3, which is DFT-D3 correction versions of M06-2X [23, 24]. The M06-2X (hybrid meta-GGA exchange-correlation functional) is a high-nonlocality functional with double the amount of nonlocal exchange (2X) for nonmetals. The triple-zeta 6-311+G (d, p) split valence-shell basis set augmented by d-polarization functions on heavy atoms and p-polarization functions on hydrogen atoms as well as diffuse functions for heavy atoms was used. The basis sets are 6-311+G (d, p), which were found suitable for biomolecules [25]. The tight convergence criterion of Gaussian 09 was used in structure optimization, and the ultrafine integration grid was used in the numerical integration of the structure optimization and vibrational frequencies calculation. Since the X-ray structures of GAs and GOA studied in this work can not be

obtained from the databases, the rotamers whose rotating dihedral angles are C20-C22-C23-C24 and C23-C24-C25-C26 were constructed as the initial structures in the geometry optimization. The geometries of GAs and GOA were fully optimized without any constraint on the geometry and the optimized structure had no imaginary frequency. For each molecule, the rotational isomer with the minimum energy was adopted for spectral calculations. The harmonic vibrational frequency scaling factor used for M06-2X-D3/6-311+G(d, p) is 0.9603 [26]. Then the calculated activities were converted using the following relationship derived from the basic theory of Raman scattering [27, 28]: $I_i = f(\nu_0 - \nu_i)^4 A_i/\nu_i\,[1 - exp(-hc\nu_i/kT)]$, where ν_0 is the exciting frequency (in unit of cm^{-1}), ν_i is the vibrational frequency (in unit of cm^{-1}) of the *i*th normal mode, *h*, *c*, and *k* are fundamental constants, and *f* is a suitably chosen common normalization factor for all peak intensities. Vibrational frequency assignments were made based on the results of the Gaussview program 5.0.8 version [29]. The Cartesian displacements of the calculated vibrational modes of GAA and GOA were also obtained from the Gaussview program.

4 Results and discussion

4.1 Structure of GAA

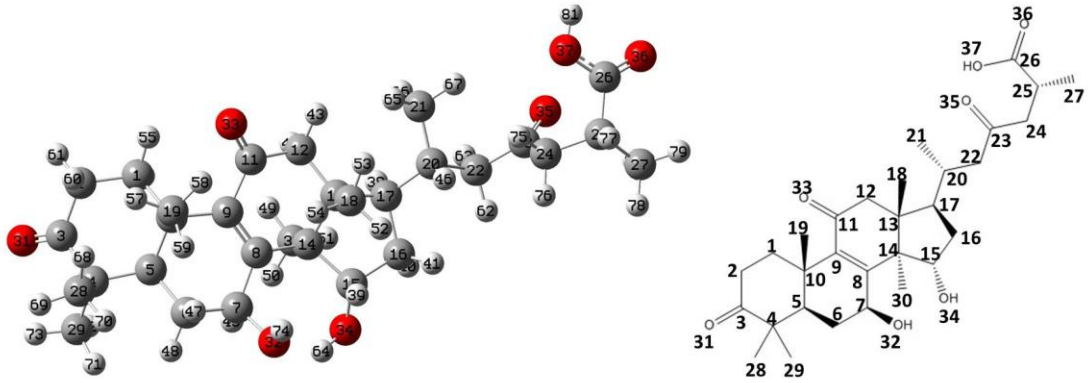

Figure 1. 3D optimized structure, 2D structure diagram, and labeling of atoms in GAA.

The optimized structure and labeling of GAA whose molecular formula is $C_{30}H_{44}O_7$ are shown in Figure 1. The labeling of GAA is basically consistent with the previous work on GAA [8]. The total charge of GAA is zero, and the spin multiplicity is 1. The atomic coordinates of GAA are displayed in the Table S1 (in Supporting Information). It comprises three six-member rings (ring 1, ring 2, ring 3) named as R1, R2, R3, and one five-member ring (ring 4) named as R4. R1 is made up of atoms C1-C2-C3-C4-C5-C10, R2 is made up of atoms C5-C6-C7-C8=C9-C10, R3 is made up of atoms C8=C9-C11-C12-C13-C14, R4 is made up of atoms C13-C14-C15-C16-C17, respectively. The label number of the atoms in GAA, and their dependent bond lengths, angles and dihedral angles are all listed in the Table S2. The bond lengths of C-H bonds are about 1.09 Å, the bond lengths of O-H bonds are about 0.96 Å, the bond length of C=C double bond is about 1.36 Å, the

bond lengths of C=O double bonds are about 1.22 Å, the bond lengths of C-C singlet bonds are about 1.5 Å to 1.6 Å, the bond lengths of C-O singlet bonds are about 1.35 Å to 1.5 Å.

4.2 IR and Raman spectra of GAA

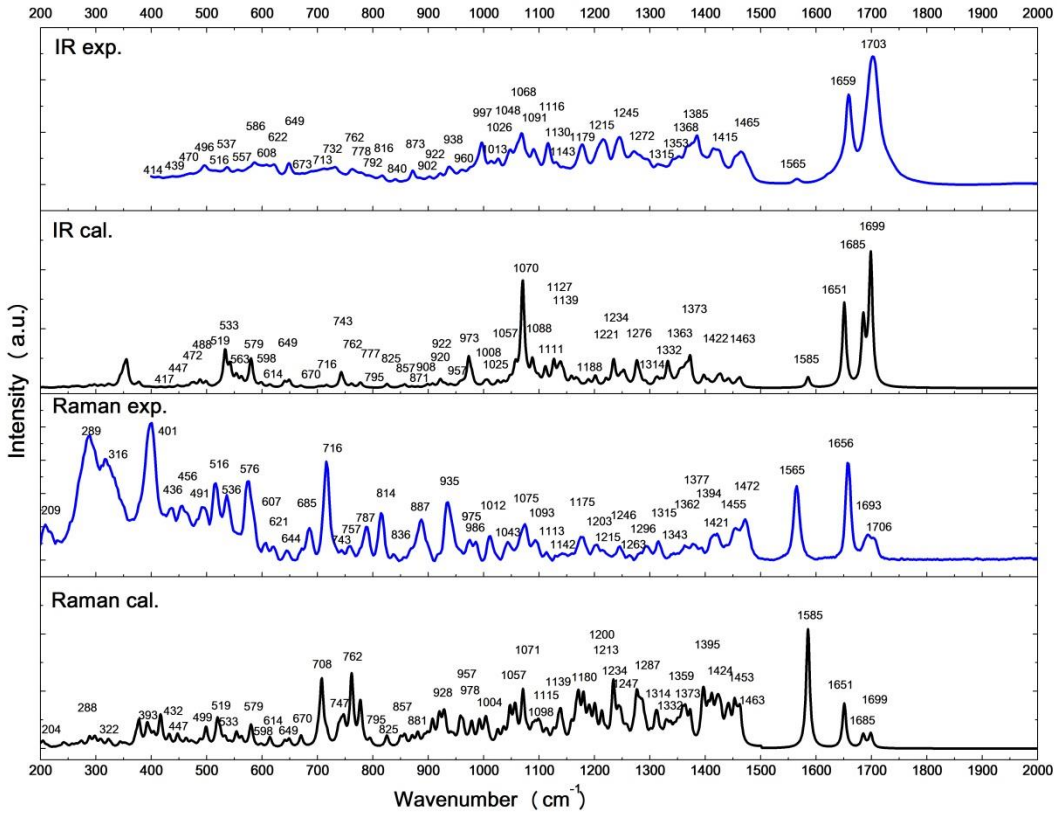

Figure 2. The experimental (blue line) and calculated (black line) of IR and Raman spectra of GAA.

The calculated IR and Raman spectra of GAA are compared with the experimental spectra in Figure 2, most of the wavenumbers and intensities of the bands are well matched. Therefore, the vibration modes can be well identified and analyzed based on the experimental and calculated Raman spectra. Simultaneous analysis of IR and Raman spectra can promote the vibration mode assignments more accurate, reliable and comprehensive. Since many bands have strong IR intensity but weak Raman intensity like 1703 cm^{-1} band in experimental IR spectrum; or have strong Raman intensity but weak IR intensity like 1565 cm^{-1} and 716 cm^{-1} bands in the experimental Raman spectrum. The vibrational frequencies, experimental Raman intensities, simulated Raman scattering activities and assignments of these bands between 200 to 2000 cm^{-1} are listed in **Table 1**.

In the region of 1500-1800 cm^{-1} in both IR and Raman spectra, there are several strong bands which stem from the stretching vibrational modes of duplet bonds, and the positions and intensities of these bands are in very good agreement with the simulated spectra. With the help of calculated spectra, we can infer that the weak 1565 cm^{-1} band in the experimental IR spectrum and the strong 1565 cm^{-1} band in the experimental Raman spectrum are from the same vibrational modes which are related to the stretching vibrational mode of C8=C9 duplet bonds. The strong 1659 cm^{-1} IR band

and the strong 1656 cm^{-1} Raman band are from the same vibrational mode which is the stretching vibrational mode of C11=O33 duplet bonds. The strong 1703 cm^{-1} IR band and the weak 1706 cm^{-1} Raman band are from the same vibrational mode which is the stretching vibrational mode of C26=O36 and C23=O35 duplet bonds. The weak band 1693 cm^{-1} Raman band is from the stretching vibrational mode of C3=O31, and we can infer that the corresponding experimental IR band may be covered by the strong 1703 cm^{-1} band.

In the 1200-1500 cm^{-1} region, many bands are from the vibrational modes of C-H bonds or O-H bond. The 1465 cm^{-1} IR band (corresponding to 1472 cm^{-1} Raman band), the 1385 cm^{-1} IR band (corresponding to 1377 cm^{-1} Raman band), the 1415 cm^{-1} IR band and the 1455 cm^{-1} and 1421 cm^{-1} experimental Raman bands are mainly from the scissoring vibration of $-CH_3$ groups (methyl groups). The 1362 cm^{-1} Raman band is from the symmetry bending vibration of $-CH_3$ groups (methyl groups). The 1368 cm^{-1} IR band and 1287 cm^{-1} Raman band are mainly from wagging vibration of $-CH_2-$ groups (methylene groups). The 1394 cm^{-1} Raman band is from the bending vibration of -CH- groups (methenyl groups). The 1215 cm^{-1} IR band is mainly from the bending vibration of O32-H, and 1263 cm^{-1} experimental Raman band is mainly from the bending vibration of O34-H and O37-H bonds. The 1245 cm^{-1} experimental IR band (corresponding to 1246 experimental Raman band) is from bending vibration of O34-H and the asymmetry stretching vibration of C13-C14, C12-C13 bonds. The exception is that the 1272 cm^{-1} experimental IR band is mainly from the stretching vibration of C9-C11 bond. This band is blue-shifted relative to other C-C single bonds due to the influence of the adjacent double bond (C11=O33, C8=C9).

The intensities of the IR bands in the 600 - 1200 cm^{-1} region are rather weak; therefore, it is difficult to analyze the vibration modes/bands if only from the experimental IR spectrum. But the Raman spectrum in this region is rather strong since the Raman spectrum measured by our 785 nm laser is very sensitive at low wavenumbers. Therefore, the combination of the two spectra can reasonably analyze the vibration modes of GAA. In the 600 - 1200 cm^{-1} region, most bands are from the vibrational modes of C-C single bonds (including breathing and deformation modes of the six-membered rings and five-membered ring) or C-O single bonds. But there are also exceptions. The 1026 cm^{-1}, 1013 cm^{-1} IR bands and 1012 cm^{-1} Raman band are from the wagging vibration of the $C-CH_3$ groups (methyl groups). The 762 cm^{-1} IR band (corresponding to 757 cm^{-1} Raman band) is mainly from the symmetry stretching vibration of C26=O37 and C26=O36, combining with the symmetry stretching vibration of C25-C26, C25-C24 and C25-C27. The 713 cm^{-1} IR band is mainly from the out of plane bending of C3, and the deformation of ring 1. The 649 cm^{-1} IR band (corresponding to 644 cm^{-1} Raman band) is from bending of C20-C22-C23, C12-C11=O33 and C24-C23-O35.

In the 200 cm^{-1} to 600 cm^{-1} region, most bands are from the bending vibrational modes of the groups. The 586 cm^{-1} IR band (corresponding to 576 cm^{-1} Raman band) is mainly from the out-of-plane bending vibration of C26=O37-H. The 557 cm^{-1} IR band and 537 cm^{-1} IR band (corresponding to 536 cm^{-1} Raman band) are mainly from the out-of-plane bending vibration of C15-O34-H. The

IR and Raman bands in the 350-460 cm^{-1} region are from the out-of-plane bending of carbon atom (including the rings). The 204 cm^{-1}, 288 cm^{-1}, 322 cm^{-1} Raman bands are mainly from the twisting of the C-CH_3 groups (methyl groups).

Table 1. Comparison between the experimental and calculated IR and Raman spectrum of GAA at M06-2X-D3/6-311+G(d,p) level. Calculated and experimental IR and Raman frequencies (cm^{-1}), simulated Raman scattering activity (R_A $Å^4$/amu), experimental Raman Intensity (R_I, cps).

IR exp. (cm^{-1})	IR exp. Int.	IR cal. (cm^{-1})	IR cal. Int.	Raman exp. (cm^{-1})	Raman exp. Int.	Raman cal. (cm^{-1})	Raman scattering activity	Assignment
1703	1.227	1699	1273.585	1706	1285.103	1699	78.196	str C26=O36, strC23=O35
		1685	622.127	1693	1539.774	1685	71.224	str C3=O31
1659	0.862	1651	823.813	1656	5850.428	1651	236.535	str C11=O33
1565	0.054	1585	102.626	1565	4455.124	1585	610.326	str C8=C9
1465	0.315	1463	39.797	1472	2454.162	1463	29.332	sci C19H_3, sci C28H_3
		1453	4.889	1455	1939.014	1453	32.229	sci C30H_3
		1424	10.727	1421	1595.982	1424	14.031	sci C27H_3
1415	0.346	1422	17.398			1422	7.614	sci C29H_3, sci C19H_3
		1395	9.067	1394	748.997	1395	22.764	bend C15H, bend C15-O34-H
1385	0.470	1373	81.866	1377	972.973	1373	21.652	sci C24H_2, sym bend C18H_3, sym bend C30H_3
1368	0.371	1363	38.234			1363	4.339	wag C24H_2, str C23-C24, sym bend C18H_3
		1359	17.695	1362	889.950	1359	16.461	sym bend C30H_3, sym bend C19H_3, sym bend C28H_3
1353	0.270	1332	114.182	1343	434.858	1332	8.529	str C26-O37, bend O37-H, sym bend C27H_3, bendC25-H
1315	0.196	1314	28.593	1315	1147.221	1314	17.282	bend C15-H, bend C20-H, bend C7-H
		1287	2.026	1296	838.505	1287	23.699	wag C6H_2, wag C1H_2
1272	0.317	1276	114.413			1276	33.571	str C9-C11, wag C22H_2, bend C7H, twist C6H_2
		1247	35.631	1263	302.337	1247	17.063	bend O34-H, bend O37-H, bend C15-H, bend C25-H
1245	0.456	1234	51.735	1246	831.648	1234	36.974	bend O34-H, str C13-C14, str C12-C13, bend C15-H
1215	0.433	1221	32.075			1221	6.444	bend O32-H, bend C7-H, twist C6-H_2
		1213	1.194	1215	604.554	1213	23.024	twist C24-H_2, bend C25-H, twist C22-H_2
		1200	8.484	1203	918.208	1200	18.090	str C8-C14, str C14-C15, twist C22-H_2
1179	0.383	1188	27.202			1188	9.594	str C4-C5, str C4-C28, bend O32-H
		1180	4.145	1175	1395.407	1180	33.382	str C4-C28, str C10-C19, twist C2H_2, twist C6-H_2
1143	0.171	1139	73.876	1142	414.122	1139	19.793	str C22-C23, str C23-C24, twist C22-H_2, bend O32-H
1130	0.214	1127	112.669			1127	5.941	str C26-O37, bend O37-H, twist C24-H_2
		1115	6.053	1113	481.636	1115	6.894	str C13-C17, str C7-C8, str C17-C20
1116	0.399	1111	81.070			1111	5.409	breath ring4, str C20-C21, def ring1

		1098	29.500	1093	1208.622	1098	11.216	str C16-C17, twist $C12H_2$, str C20-C21
1091	0.338	1088	108.301			1088	9.441	str C24-C25, str C26-O37, bendO37-H, bend C25-H
		1071	59.682	1075	2173.566	1071	32.994	def ring1, def ring4, twist $C16-H_2$
1068	0.491	1070	456.771			1070	6.591	str C15-O34, breath ring4, str C26-O37
1048	0.336	1057	84.748	1043	1098.975	1057	19.238	str C7-O32, breath ring3, breath ring4, str C15-O34
1026	0.247	1025	26.067			1025	10.086	wag $C20-C21H_3$, wag $C25-C27H_3$, wag $C13-C18H_3$, wag $C13-C26H_3$
1013	0.225	1008	22.200			1008	5.524	wag $C4-C29H_3$, wag $C14-C30H_3$, wag $C13-C18H_3$, def ring1,2,3,4
		1004	8.577	1012	1439.593	1004	11.971	wag $C4-C28H_3$, wag $C4-C29H_3$, def ring 4
		978	44.180	986	1116.175	978	15.534	def ring4, str C15-C16, str C16-C17
997	0.402	973	136.819			973	1.933	breath ring 2,3,4, bend C4-C29H3
960	0.142	957	18.158	975	1220.412	957	15.706	str C17-C20, breath ring4, def ring 2,3
		928	3.771	935	3484.500	928	13.907	str C4-C28, str C4-C29, wag $C4-C28H_3$, wag $C4-C29H_3$, rock $C2H_2$, rock $C1H_2$
938	0.172	922	32.891			922	3.320	str C24-C25, wag $C25-C27H_3$
922	0.108	920	6.319			920	16.612	str C10-C19, str C14-C30, rock $C1H_2$
902	0.077	908	15.276			908	15.814	str C11-C12, str C1-C10, def ring1,2,3,4
		881	4.020	887	2448.351	881	8.655	str C13-C14, def ring 3,4, rock $C16H_2$
873	0.132	871	4.817			871	6.126	breath ring1,2,4, def ring3, rock $C12H_2$
840	0.050	857	15.464	836	345.762	857	7.070	str C20-C21, def ring 1,2,4
816	0.086	825	15.972	814	2832.999	825	4.336	str C23-C24, def ring1, rock $C22H_2$
792	0.089	795	0.691	787	2004.828	795	4.393	str C22-C23, str C23-C24, rock $C22-H_2$, rock $C24H_2$
778	0.115	777	24.377			777	26.861	str C20-C21, str C13-C18, def ring 2,3,4
762	0.148	762	16.341	757	837.358	762	43.250	sym str C26=O37, str C26=O36, sym str C25-C26, str C25-C24, str C25-C27
		747	11.605	743	607.497	747	12.381	breath ring 1,2,3,4,
732	0.168	743	72.103			743	8.267	def ring 2,3,4, bend out C26, bend $C25-C27H_3$
713	0.152	716	11.662			716	5.968	bend out C3, def ring1
		708	4.572	716	5928.517	708	38.572	breath ring1, def ring2
673	0.108	670	9.340	685	1929.474	670	6.703	def ring 1,2,4, breath ring3
649	0.205	649	34.510	644	565.378	649	4.396	bend C20-C22-C23, bend C12-C11=O33, bend C24-C23-O35, bend out C26
622	0.192	614	12.898	621	803.032	614	5.798	def ring 1,4, rock $C12H_2$
608	0.191	598	19.507	607	1041.799	598	1.522	def ring 3, breath ring1
586	0.212	579	74.368	576	4742.559	579	6.448	bend out C26=O37-H, def ring1
557	0.141	563	37.612			563	4.484	bend out C15-O34-H, def ring 1,3,4
537	0.167	533	172.127	536	3914.758	533	4.087	bend out C15-O34-H, bend out C26=O37-H

516	0.135	519	5.206	516	4623.203	519	12.848	def ring2,3,4, bend C22-C23=O35
		499	26.083	491	3178.976	499	9.667	bend out C15-O34-H, def ring 2,4
496	0.185	488	34.174			488	2.921	bend C25-C26=O37, rock $C16H_2$
470	0.107	472	14.243			472	2.135	bend C25-C26=O37, rock $C24H_2$, rock $C16H_2$
439	0.079	447	10.522	456	3261.670	447	5.709	twist C17-C20-C22-C23, twist out ring 2,3,4, rock $C24H_2$
		432	4.171	436	3123.473	432	5.131	twist ring2,3
414	0.075	417	2.694			417	12.964	bend out C25, bend C22-C23=O35
		393	2.271	401	8248.754	393	8.624	twist ring 2,4
		322	12.500	316	6065.568	322	2.617	twist $C25\text{-}C27H_3$, bend C22-C23-C24
		288	9.395	289	7509.488	288	3.536	twist $C14\text{-}C30H_3$, twist $C13\text{-}C18H_3$, twist $C20\text{-}C21H_3$
		204	2.703	209	2139.973	204	1.810	twist $C4\text{-}C28H_3$, twist $C10\text{-}C19H_3$, twist $C14\text{-}C30H_3$

Bend, bending; breath, breathing; def, in-plane deformation; def-out, out of plane deformation, rock, rocking; sci, scissoring; str, stretching; twist, twisting; twist out, out of plane twisting ; wag, wagging; sym, symmetry; asym, asymmetry; R1, ring 1; R2, ring2; R3 ring 3; R4, ring 4. The label numbers of hydrogen atoms are not listed, subscript 1, 2, and 3 refer to the number of hydrogen atoms.

4.3 Distinguish the type of GAs by IR and Raman spectra

Besides GAA, there are many other ganoderic acids such as ganoderic acid B (GAB), ganoderic acid C (GAC) and ganoderic acid D (GAD), as shown in Figure 3. Their main difference is that their functional groups are different. Because, in different type of ganoderic acid, the groups at positions C3, C7, C12, C15, C22, C23 may be hydrogen atom, hydroxyl groups, ketones (C=O) or acetoxy group (-O-CO-CH_3), as shown in Figure 3 [5, 8, 16]. The IR or Raman intensity of bands from C=O groups are always rather strong at in the 1500 cm^{-1} to 1800 cm^{-1} region. Therefore, the IR and Raman spectra in this region can be used to distinguish the type of ganoderic acids. The simulated spectra and of GAs and experimental spectra of GAA are compared in Figure 4, and the assignment of these bands are listed in **Table 2**.

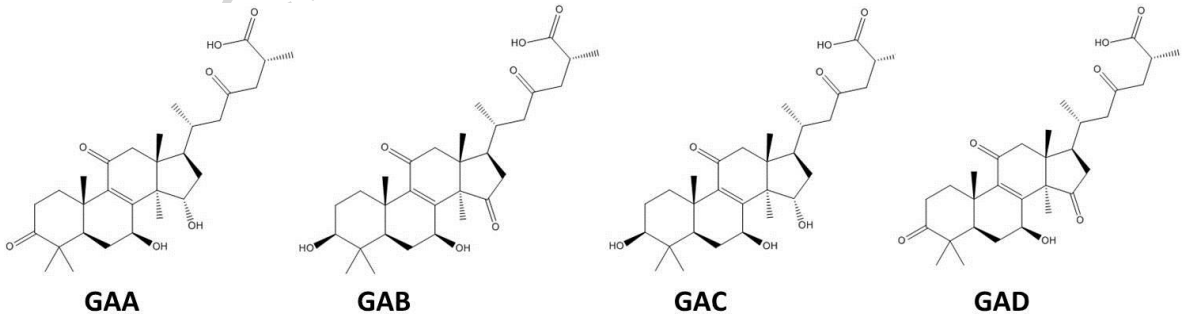

Figure 3. The 2D Structure diagram of GAA, GAB, GAC and GAD.

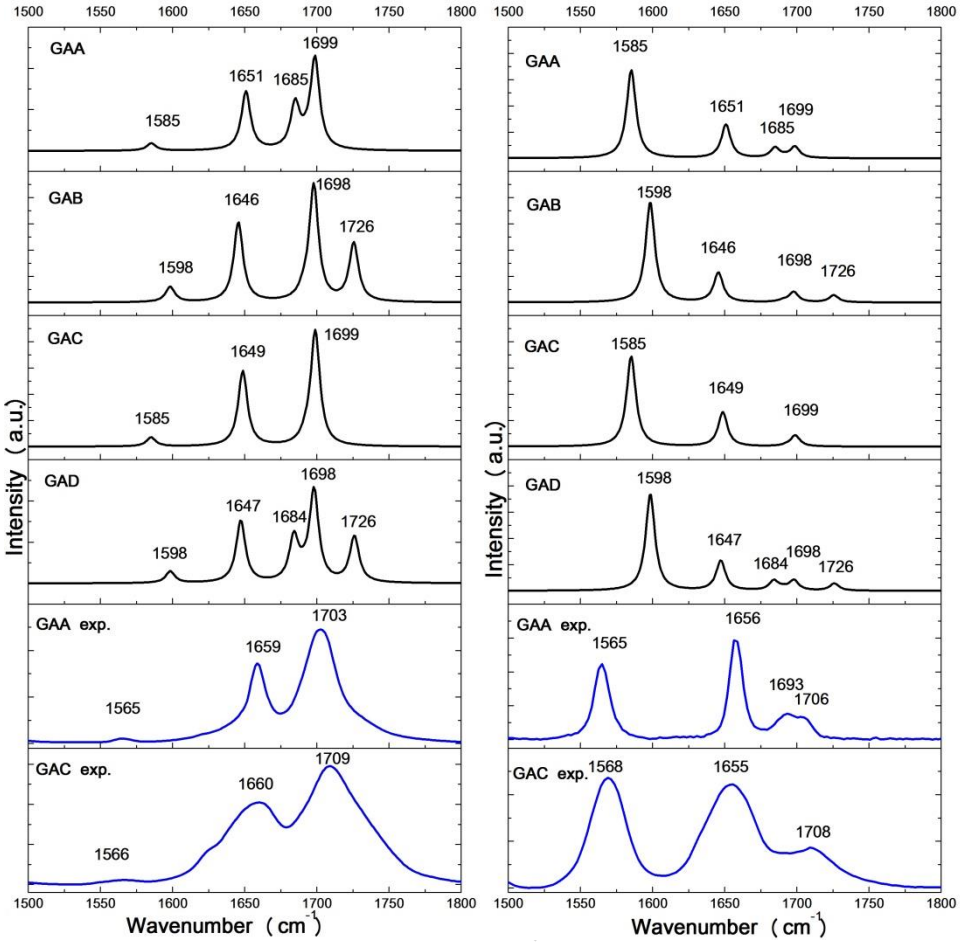

Figure 4. Black: the simulated (left) IR and (right) Raman spectra of GAA, GAB, GAC and GAD. Blue: the experimental (left) IR and (right) Raman spectra of GAA and GAC.

Table 2. Comparison of the simulated wavenumbers (cm^{-1}) of GAA, GAB, GAC and GAD at M06-2X-D3/6-311+G(d,p) level in 1500 cm^{-1} to 1800 cm^{-1} region.

GAA	GAB	GAC	GAD	assignment
	1726		1726	str C15=O34
1699	1698	1699	1698	str C26=O36, str C23=O35
1685			1684	str C3=O31
1651	1646	1649	1647	str C11=O33
1585	1598	1585	1598	str C8=C9

In the simulated spectra of GAs, it's found that the bands from the same vibrational mode have similar wavenumbers. For instance, the strong IR band of GAs from the stretching vibrational mode of C26=O36 and C23=O35 duplet bonds are located at 1698 cm^{-1} and 1699 cm^{-1}. And the biggest difference is only 14 cm^{-1} which is from the stretching vibrational mode of C8=C9 duplet bonds. Therefore, from the IR and Raman bands we can infer the corresponding group and determine the type of the GAs. For instance, in Figure 4, the sample not having experimental IR and Raman band at about 1726 cm^{-1} means that there is not C15=O34 group at C15 site and it cannot be GAB or GAD. The existence of the Raman band at about 1693 cm^{-1} means the existence of C3=O31 group and it can be GAA or GAD. From these two points we can identify the sample GAA. On the other hand, as shown in Figure 4, it is not easy to distinguish GAA and GAC if only based on the IR spectra, because the corresponding experimental IR band of GAA is covered by the strong band at 1703 cm^{-1}. In order to distinguish GAA and GAC, both IR and Raman spectra of GAC are compared (spectra in 200-2000 cm^{-1} region are shown in Figure S1). With the comparison of Raman bands in the 1690 -1710 cm^{-1} region, we can easily identify GAA from GAC for there is only one weak band at 1704 cm^{-1} for GAC, but there are two weak bands at 1693 cm^{-1} and 1706 cm^{-1} for GAA. Therefore, the employment of both IR and Raman spectra can help to distinguish different GAs.

4.4 GAA and GOA

Besides, Ganoderenic acids (Ganoderenic acid A, GOA, Ganoderenic acid B, GOB, et al.) can also be extracted from the *Ganoderma lucidum* [16, 21, 30, 31]. And some works report that Ganoderenic acids (GOs) have a similar pharmacological effect with GAs [21, 30, 32]. The only difference between GOs and GAs is the formation of C20=C22 double bond by dehydrogenation of GAs. Therefore, combination of both IR spectroscopy and Raman spectroscopy may also be useful for identifying GOs in contrast with their corresponding GAs.

Based on the approach explained above, we could also analyze the vibrational spectra of Ganoderenic acid A (GOA). The optimized structure and atom labeling of GOA whose molecular formula is $C_{30}H_{42}O_7$ are shown in Figure 5. It is therefore necessary to use spectral methods to distinguish between these two very similar compounds. The experimental and calculated infrared and Raman spectra of these two compounds were simultaneously compared, as shown in Figures 6 and 7, respectively.

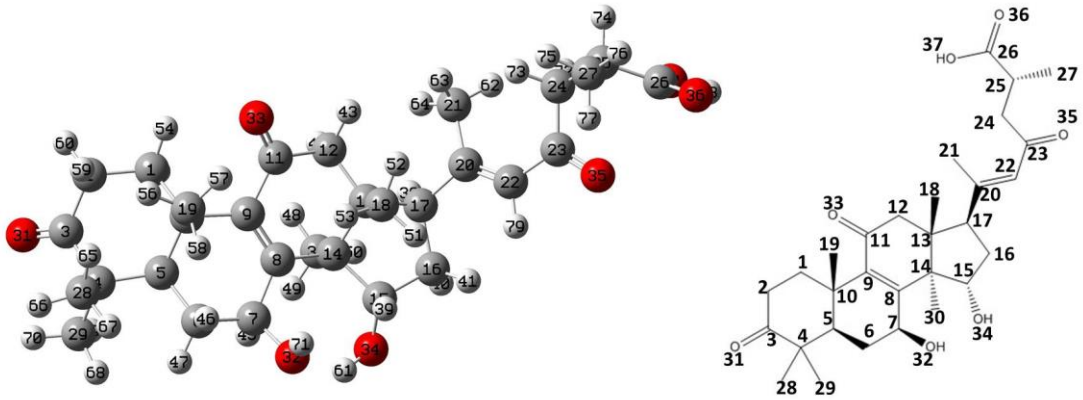

Figure 5. Labeling of atoms in Ganoderenic acid A (GOA).

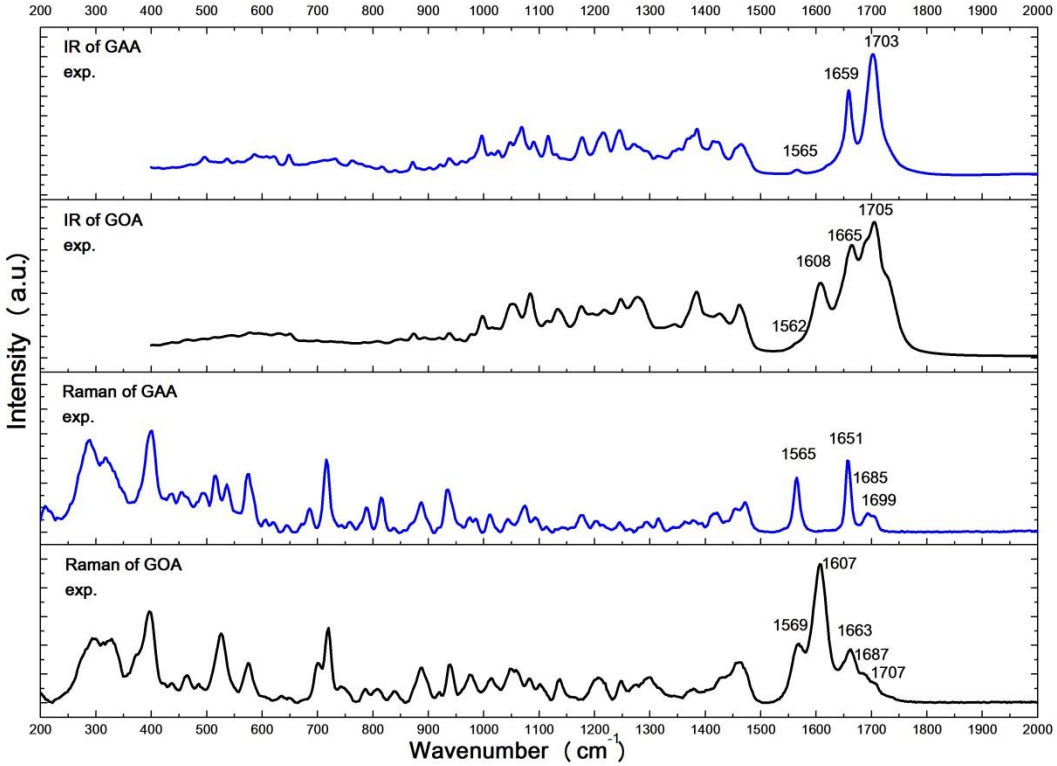

Figure 6. The experimental IR and Raman spectra of GAA and GOA.

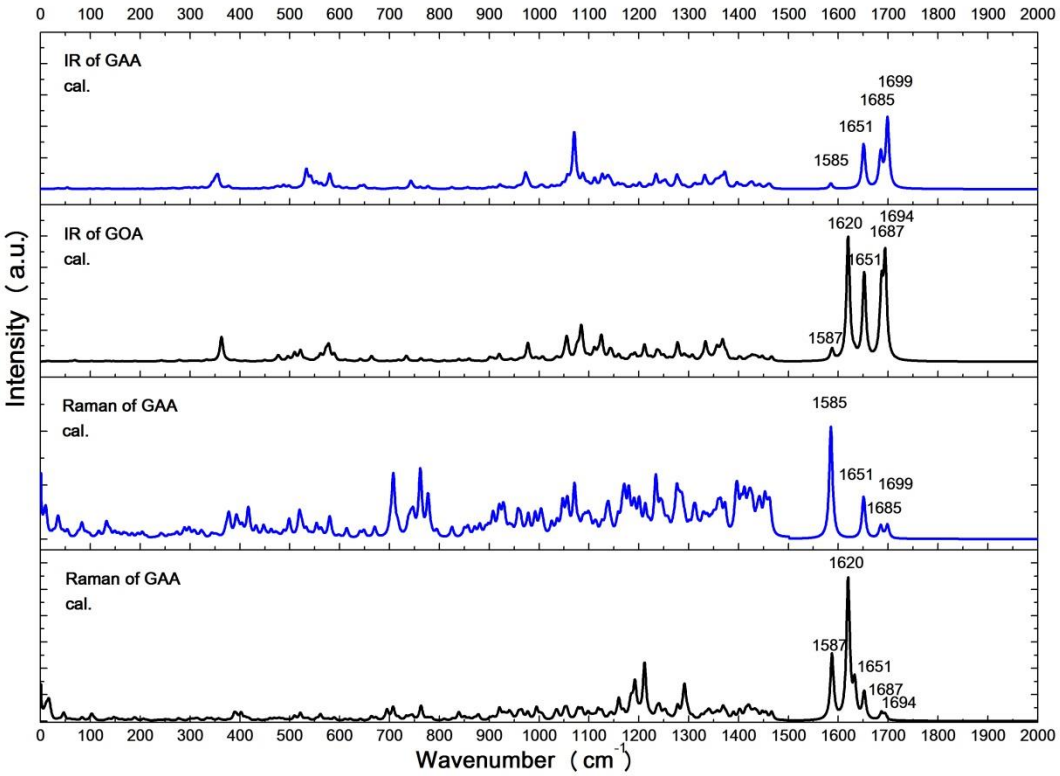

Figure 7. The simulated IR and Raman spectra of GAA and GOA.

In Figure 6, the most obvious difference between spectra of GOA and GAA is located at the region from 1500 cm^{-1} to 1800 cm^{-1}. For GOA, a strong new IR band appears at 1608 cm^{-1}, meanwhile a strong new Raman band appears at 1607 cm^{-1}. Compared with the simulated spectra in Figure 7, a new IR band and a new Raman band at 1620 cm^{-1} can be identified. The new IR and Raman experimental band is from the same vibration mode, which is mainly from the in phase stretching vibration of the C20=C22 and C23=35, as shown in Figure S2 in the Supporting Information. There are also many other Ganoderenic acids like GOB, GOC, GOD, GOE which also contains a C20=C22 carbon-carbon double bond on the side chain comparing with the corresponding Ganoderic acid. Therefore, through this IR/Raman band at about 1620 cm^{-1}, we can identify whether it is Ganoderenic acid or ganoderic acid. In the region from 1500 cm^{-1} to 1800 cm^{-1}, despite the difference of this band, the other bands of GAA and GOA have almost the same positions and intensities. Contrast to the corresponding GAs, the GOs should also have similar bands in the region from 1500 cm^{-1} to 1800 cm^{-1}. Therefore, we can also determine the type of the GOs through the comparison of IR/Raman spectra.

5 Conclusions

In this work, we conducted investigated the vibrational properties of some Ganoderic acids and especially Ganoderic acid A. We measured the IR and Raman spectra of GAA, and with the use of the density functional theory calculation, we optimized the molecular structure of GAA and simulated its corresponding IR and Raman spectra. Furthermore, based on the analysis of the

spectral region of 1500-1800 cm^{-1}, different types of GAs (for instance GAA, GAB, GAC, GAD) can also be distinguished. In addition, the IR and Raman spectra of similar compounds GOA were also compared. As a result, we showed that GOA could also be distinguished from GAA due to the strong band from the vibration mode of the alkene in GOA. As such, we believe that this work has provided the first detailed IR/Raman spectral study, which may also practically useful for the application of IR/Raman spectroscopy in the inspection and quality control of *Ganoderma lucidum*.

Acknowledgements

This work was supported by the National Natural Science Foundation of China (No. 11635013, No. 11775272 and No. 11475217) and the Strategic Priority Research Program of the Chinese Academy of Sciences (No. XDA08040107).

References

[1] M.S. Shiao, K.R. Lee, L.J. Lin, C.T. Wang, Food Phytochemicals for Cancer Prevention Ii, 547 (1994) 342-354.

[2] K.S. Bishop, C.H.J. Kao, Y.Y. Xu, M.P. Glucina, R.R.M. Paterson, L.R. Ferguson, Phytochemistry, 114 (2015) 56-65.

[3] C.J. Weng, C.F. Chau, G.C. Yen, J.W. Liao, D.H. Chen, K.D. Chen, Journal Of Agricultural And Food Chemistry, 57 (2009) 5049-5057.

[4] D. Sliva, Mini-Reviews In Medicinal Chemistry, 4 (2004) 873-879.

[5] J.W. Xu, W. Zhao, J.J. Zhong, Applied Microbiology And Biotechnology, 87 (2010) 457-466.

[6] Q.X. Yue, Z.W. Cao, S.H. Guan, X.H. Liu, L. Tao, W.Y. Wu, Y.X. Li, P.Y. Yang, X. Liu, D.A. Guo, Molecular & Cellular Proteomics, 7 (2008) 949-961.

[7] E.S. Petrova, M.I. Rudina, Y.S. Shvarts, Pharmaceutical Chemistry Journal, 52 (2018) 57-62.

[8] T. Kubota, Y. Asaka, I. Miura, H. Mori, Helvetica Chimica Acta, 65 (1982) 611-619.

[9] S. Fatmawati, K. Shimizu, R. Kondo, Fitoterapia, 81 (2010) 1033-1036.

[10] H. Hajjaj, C. Mace, M. Roberts, P. Niederberger, L.B. Fay, Applied And Environmental Microbiology, 71 (2005) 3653-3658.

[11] S.K. Eo, Y.S. Kim, C.K. Lee, S.S. Han, Journal Of Ethnopharmacology, 68 (1999) 129-136.

[12] N. Sato, Q. Zhang, C.M. Ma, M. Hattori, Chemical & Pharmaceutical Bulletin, 57 (2009) 1076-1080.

[13] G.S. Wu, J.J. Lu, J.J. Guo, Y.B. Li, W. Tan, Y.Y. Dang, Z.F. Zhong, Z.T. Xu, X.P. Chen, Y.T. Wang, Fitoterapia, 83 (2012) 408-414.

[14] J.S. Zhou, S.L. Ji, M.F. Ren, Y.L. He, X.R. Jing, J.W. Xu, Biochemical Engineering Journal, 90 (2014) 178-183.

[15] Q. Luo, X.L. Wang, L. Di, Y.M. Yan, Q. Lu, X.H. Yang, D.B. Hu, Y.X. Cheng, Tetrahedron, 71 (2015) 840-845.

[16] D.H. Chen, W.K.D. Chen, Journal Of Food And Drug Analysis, 11 (2003) 195-200.

[17] B.S. Gill, Navgeet, R. Mehra, V. Kumar, S. Kumar, Investigational New Drugs, 36 (2018) 136-143.

[18] F.R. Cao, B.X. Xiao, L.S. Wang, X. Tao, M.Z. Yan, R.L. Pan, Y.H. Liao, X.M. Liu, Q. Chang, Journal Of Chromatography B-Analytical Technologies In the Biomedical And Life Sciences, 1052 (2017) 19-26.

[19] T. Akihisa, Y. Nakamura, M. Tagata, H. Tokuda, K. Yasukawa, E. Uchiyama, T. Suzuki, Y. Kimura, Chemistry & Biodiversity, 4 (2007) 224-231.

[20] J. Zhu, J. Jin, J. Ding, S. Li, P. Cen, K. Wang, H. Wang, J. Xia, Chem Biol Interact, 290 (2018) 77-87.

[21] R.L. Zhao, Y.M. He, Journal Of Ethnopharmacology, 210 (2018) 287-295.

[22] M.J. Frisch, G.W. Trucks, H.B. Schlegel, G.E. Scuseria, M.A. Robb, J.R. Cheeseman, G. Scalmani, V. Barone, B. Mennucci, G.A. Petersson, H. Nakatsuji, M. Caricato, X. Li, H.P. Hratchian, A.F. Izmaylov, J. Bloino, G. Zheng, J.L. Sonnenberg, M. Hada, M. Ehara, K. Toyota, R. Fukuda, J. Hasegawa, M. Ishida, T. Nakajima, Y. Honda, O. Kitao, H. Nakai, T. Vreven, J.A. Montgomery, Jr., J.E. Peralta, F. Ogliaro, M. Bearpark, J.J. Heyd, E. Brothers, K.N. Kudin, V.N. Staroverov, R. Kobayashi, J. Normand, K. Raghavachari, A. Rendell, J.C. Burant, S.S. Iyengar, J. Tomasi, M. Cossi, N. Rega, N.J. Millam, M. Klene, J.E. Knox, J.B. Cross, V. Bakken, C. Adamo, J. Jaramillo, R. Gomperts, R.E. Stratmann, O. Yazyev, A.J. Austin, R. Cammi, C. Pomelli, J.W. Ochterski, R.L. Martin, K. Morokuma, V.G. Zakrzewski, G.A. Voth, P. Salvador, J.J. Dannenberg, S. Dapprich, A.D. Daniels, Ö. Farkas, J.B. Foresman, J.V. Ortiz, J. Cioslowski, D.J. Fox, Gaussian 09, D. 01, in, Gaussian, Inc., Wallingford CT, 2009.

[23] Y. Zhao, D.G. Truhlar, Theoretical Chemistry Accounts, 120 (2008) 215-241.

[24] Y. Zhao, D.G. Truhlar, Journal Of Physical Chemistry C, 112 (2008) 4061-4067.

[25] G.H. Yao, Z.M. Zhai, J. Zhong, Q. Huang, Journal Of Physical Chemistry C, 121 (2017) 9869-9878.
[26] M.L. Laury, M.J. Carlson, A.K. Wilson, Journal Of Computational Chemistry, 33 (2012) 2380-2387.
[27] M. Muniz-Miranda, C. Gellini, M. Pagliai, M. Innocenti, P.R. Salvi, V. Schettino, Journal Of Physical Chemistry C, 114 (2010) 13730-13735.
[28] V. Krishnakumar, G. Keresztury, T. Sundius, S. Seshadri, Spectrochimica Acta Part a-Molecular And Biomolecular Spectroscopy, 68 (2007) 845-850.
[29] R. Dennington, T. Keith, J. Millam, GaussView 5, in, Semichem Inc., Shawnee Mission, KS, 2009.
[30] S. Fatmawati, K. Shimizu, R. Kondo, Planta Med, 76 (2010) 1691-1693.
[31] C.R. Cheng, Y.F. Li, P.P. Xu, R.H. Feng, M. Yang, S.H. Guan, D.A. Guo, Food Chemistry, 130 (2012) 1010-1016.
[32] D.H. Kim, S.B. Shim, N.J. Kim, I.S. Jang, Biological & Pharmaceutical Bulletin, 22 (1999) 162-164.

Graphic abstract

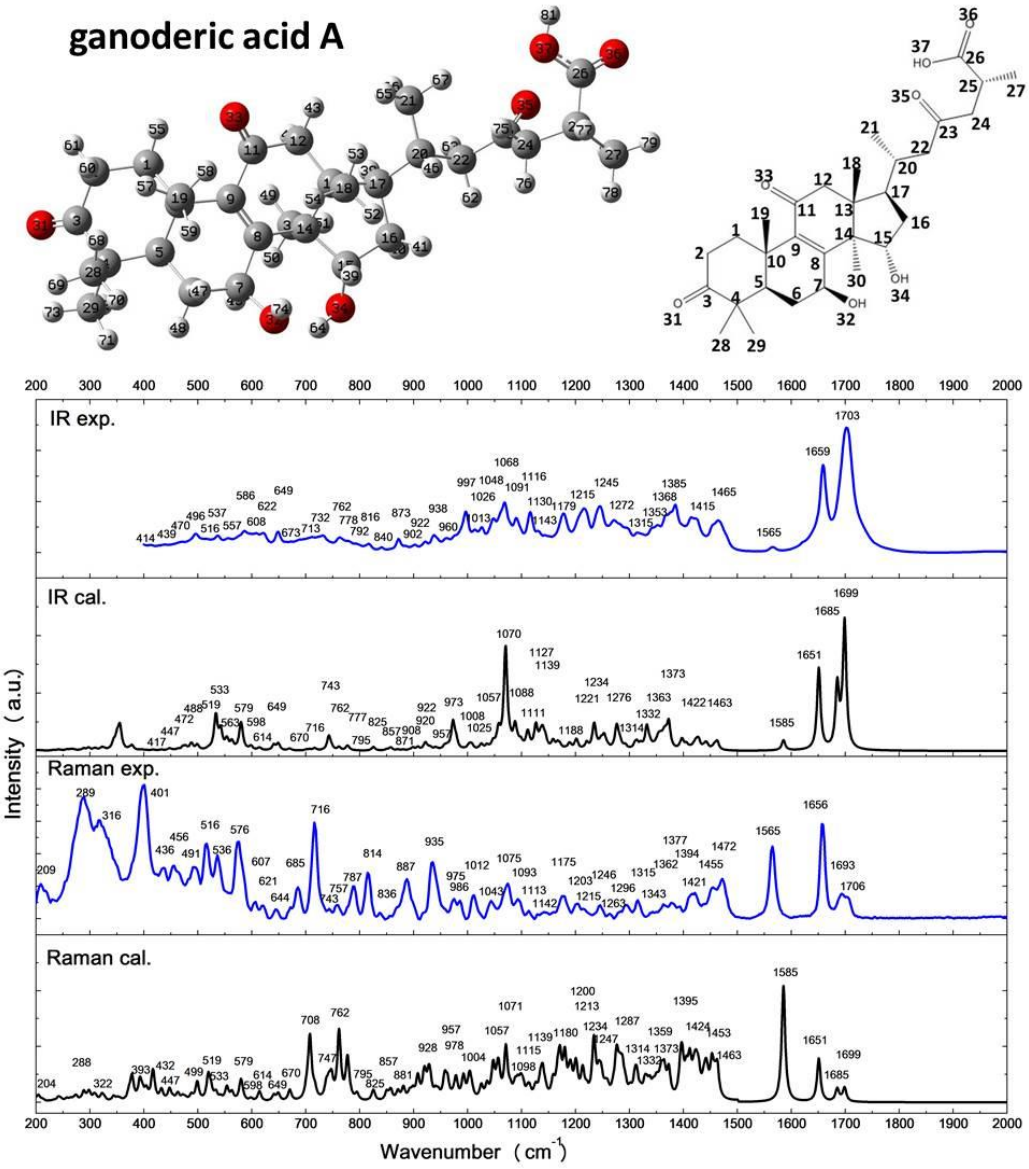

Highlights

1. The IR and Raman spectra of ganoderic acid A (GAs) are measured and computed.
2. The DFT simulation using M06-2X-D3 functionals is commendable for spectral analysis.
3. Different types of GAs can be distinguished by analysis of IR and Raman spectra.
4. Ganoderenic acid A (GOA) can also be analyzed based on the same spectral analytical approach.